Effect of the model's geometry in fretting fatigue life prediction

J. Vázquez, C. Navarro, J. Domínguez
Departamento de Ingeniería Mecánica, Universidad de Sevilla,
E.T.S.I. Camino de los Descubrimientos s/n, c.p. 41092, Sevilla, España
jesusvaleo@us.es, cnp@us.es, jaime@us.es

ABSTRACT. This paper analyses the influence that the type of geometry used to obtain the stress/strain fields in a cylindrical contact has on fretting fatigue life predictions. In addition, this work considers the effect that the fatigue crack shape assumed has on these fretting fatigue life predictions. The strain/stress fields are calculated using a series of finite elements models that consider the following three types of behaviour: plane stress, plane strain (2D geometries) and 3D. Each of these models gives a different crack initiation life and a different evolution of the stress intensity factor (SIF), which are calculated using the weight function method. These models therefore provide different fretting fatigue life predictions. Finally, the lives obtained using the numerical models are compared with experimental lives.

KEYWORDS. Fretting fatigue; Geometrical effects; Fatigue life model.

INTRODUCTION

Fretting is a superficial damage phenomenon that is found in certain mechanical joints when are subjected to fluctuating loads. Consequently, time variable contact stress distributions arise at the contacting surfaces, potentially leading to surface crack formation [1]. If there is a bulk tension at the joint in addition to the contact stress field, surface cracks may cause mechanical failure at the joint [2]. This phenomenon is referred to as fretting fatigue. Because the most common form of transmitting forces between solids is mechanical contact, fretting or fretting fatigue is present in a wide variety of mechanical components. Due to this commonality, fretting fatigue is the focus of many studies [3-5]. With the research aim of predicting the failure of mechanical components, a series of fatigue life prediction models have been developed [6-10]. In many circumstances, these models are applied to geometries and load systems whose behaviour can be assumed to be in plane stress or plane strain conditions, as observed in 2D models with actual 3D geometries.

The focus of this work is to analyse the effect produced by the geometry of the model (2D or 3D) on fatigue life prediction. For this task, fatigue life predictions were completed over a series of experimental tests, considering both 2D and 3D models. Tests were performed using cylindrical contact in which a cylindrical element was pressed against a dog-bone type fatigue test specimen while a static normal load, N, was applied. Both components were made of Al 7075-T651 alloy. The test specimen was then subjected to a cyclic axial stress, σ, and due to the assembly used and the friction between the contact pair, generates a tangential cyclic load Q (Fig. 1). More details about the experimental set up can be found in [11].

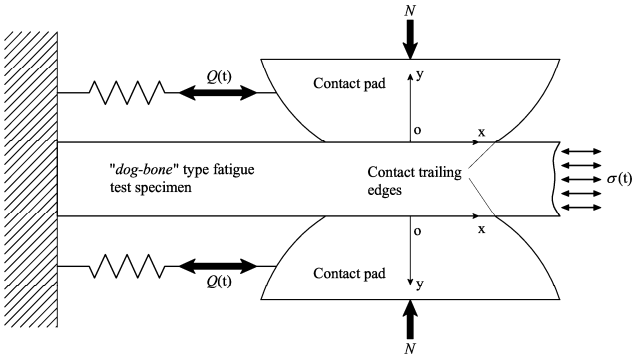

Figure 1: Scheme of the experimental assembly.

FATIGUE LIFE PREDICTION MODEL

The fretting fatigue life predictions model used in these analyses is based on a previous model proposed by the authors [7]. This model combines the crack initiation and crack propagation phases by analysing each phase independently. Using fracture mechanics procedures, the crack propagation phase is calculated using a curve. This curve offers the crack propagation cycles, $N_p(a)$, that are required to grow a crack from an initial length, a, to the final fracture crack length at which the test specimens fails. This curve is obtained by integrating the crack propagation law between a and the final crack length. Moreover, the crack initiation phase offers the number of crack initiation cycles, $N_i(a)$, required to nucleate/generate a crack of length equal to a. The $N_i(a)$ curve is obtained by considering the stress and strain fields along the prospective crack path. The total fatigue life, N_t, is obtained by adding the curves, $N_t(a)=N_i(a)+N_p(a)$. As a result, the total fatigue life, $N_t(a)$, is a function of the crack length, a, which defines when the crack initiation phase ends and the crack propagation phase begins. Depending on the value assumed for the initial crack length, a, the total fatigue life estimated is different, and the curve N_f–a can be obtained by repeating the calculation process using diverse values of a. As shown in [7], close to the contact surface the fatigue life is controlled by the crack initiation process, and far from it by the crack propagation. Therefore, the value of a that produces the minimum of the curve $N_t(a)$ is considered the nexus between the crack initiation and the crack propagation phases [8]. For this reason, and because it is the crack initiation length that offers the most conservative prediction, the minimum value of N_t is established as the fatigue life prediction.

Crack propagation phase

A fracture mechanics-based law reflecting a generic initial crack length, a, is used to calculate the crack propagation phase. Because the value of a can be measured on the order of microns, the proposed law also tries to model the short crack growth phase. For this reason, a modified threshold dependent on the actual crack length is introduced into the crack growth law [9].

$$\frac{da}{dN}=C\left(\Delta K_I^n-\left(\Delta K_{I_{th\infty}}\cdot\left(\frac{a^f}{a^f+a_0^f-l_0^f}\right)^{1/2f}\right)^n\right) \tag{1}$$

In Eq. (1), $\Delta K_{I_{th\infty}}$ is the threshold SIF range for long cracks, f is a parameter equal to 2.5 [10], l_0 is the distance between the surface and the first microstructural barrier (a grain boundary), C and n are the Paris' crack growth parameters and a_0 is the El Haddad's parameter, which is defined by

$$a_0=\frac{1}{\pi}\left(\frac{\Delta K_{I_{th\infty}}}{\Delta\sigma_{FL}}\right)^2 \tag{2}$$

in which $\Delta\sigma_{FL}$ is the stress range at the fatigue limit. The factor that multiplies $\Delta K_{I_{th\infty}}$ in Eq. (1) is based on a theoretical approximation of the Kitagawa-Takahashi diagram that considers the threshold stress to be a function of the crack length.

Many different options were considered to model the short crack growth phase [9], but it was found that one offers the best results is that shown in Eq. (1).

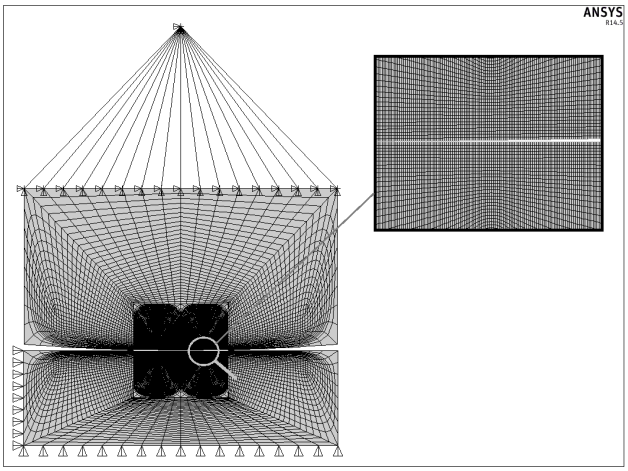

Figure 2: Mesh in the 2D models.

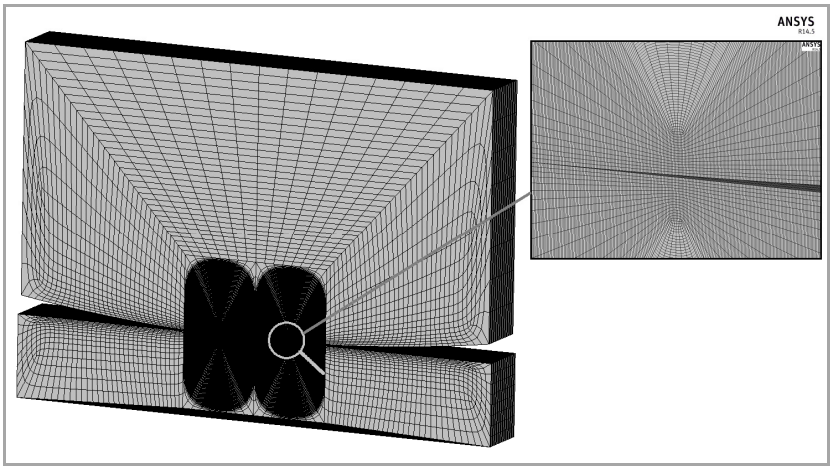

Figure 3: Mesh in the 3D models.

To study the effect exerted by the model geometry (2D or 3D) on the crack growth phase, SIF values were calculated according to the type of geometry used to model the contact pair that was used between the pad and the test specimen. In those models with a plane stress or a plane strain formulation, the SIF was obtained using the weight function proposed by Orynyak [12] and calculated as follows:

$$K_I(\phi) = \int_{\Omega} \sigma(y)\, w(g,\phi)\, dA \tag{3}$$

where Ω represents the surface crack, ϕ is the angle for a certain point along the crack front, $\sigma(y)$ is the normal stress distribution along the prospective crack faces and g symbolises the crack geometry. In the case of a 2D model, this stress distribution only varies with the y coordinate. Conversely, when a 3D model is applied, the SIF is obtained by adapting Eq. (3) to the bidimensional stress field along the crack surface:

$$K_I(\phi) = \int_{\Omega} \sigma(y,z)\, w(g,\phi)\, dA \tag{4}$$

where the normal stress $\sigma(y,z)$ is the bidimensional stress distribution on the crack surface.
Obtaining SIF using Eq. (3) and (4) is only valid until the crack becomes a through crack. From that moment forward, the SIF is calculated using the unidimensional weight function proposed by Bueckner [13]:

$$K(l)=\int_0^l \sigma(y)\, w(y,l)\, dy \tag{5}$$

In Eq. (5), σ(*y*) is the normal stress distribution along the prospective crack path. In 3D cases, this stress distribution is averaged through the test specimen thickness.

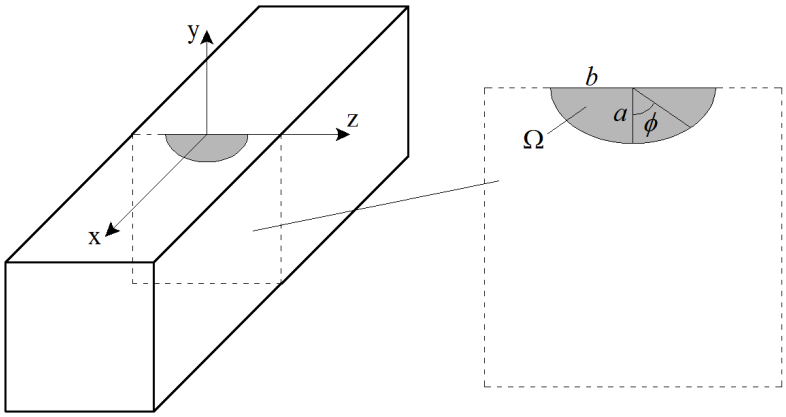

Figure 4: Crack configuration in the models.

Both stress distributions, σ(*y*) (for Eqs. (3) and (5)) and σ(), have been obtained from a series of elastic-plastic finite element analyses, which simulate the mechanical behaviour of the contact pair between the pad and the test specimen. The software used for the finite element models (FEM) was ANSYS® 14.0. Fig. 2 shows the mesh and boundary conditions used in the 2D FEM. In these cases and due to the symmetrical conditions of the actual contact pair, only half of the test specimen has been introduced into the models. In the 3D models, these symmetrical conditions allow to consider only half of the pad and a quarter of the test specimen during modelling. The FEM mesh for 3D case modelling is shown in Fig. 3. Based on experimental observation in both models (2D and 3D), the cracks have been modelled as surface cracks that are semi-elliptical and centred along the test specimen thickness and emanating from the contact trailing edge (Fig. 1 and 4).

It is further experimentally observed that the crack shape evolves as a crack grows; thus, for the SIF calculations, a variable crack aspect ratio, *b*/*a*, has been considered. The evolution of the crack aspect ratio can be obtained from the following equation:

$$\frac{\Delta b}{\Delta a}\approx\frac{db}{da}=\frac{\left(\Delta K_I^{\phi=\pi/2}(a,b/a)\right)^n-\left(\Delta K_{I_{th_\infty}}\cdot\left(\frac{a^f}{a^f+a_0^f-l_0^f}\right)^{1/2f}\right)^n}{\left(\Delta K_I^{\phi=0}(a,b/a)\right)^n-\left(\Delta K_{I_{th_\infty}}\cdot\left(\frac{a^f}{a^f+a_0^f-l_0^f}\right)^{1/2f}\right)^n} \tag{6}$$

In this equation, it is implicitly assumed that the crack grows according to the same law at the surface point ($\phi=\pi/2$) and at the deepest point ($\phi=0$) of the crack front. According to Eq. (6), the procedure used to calculate the crack aspect evolution is as follows:

1. Using the present crack length, *a*, and aspect ratio, *b*/*a*, the SIF values at the surface and the deepest point of the crack front are calculated.
2. A small crack length increment Δ*a* is imposed; in the present case, Δa =1 μm.
3. Assuming that the SIF values remain unchanged during the increment Δ*a*, Δ*b* is obtained from Eq. (6).

Suspecting that the assumed initial crack aspect ratio could have a potential influence on the *a*/*b* evolution, a series of simulations were carried out while considering different initial crack aspect ratios. The result of one of these simulations is shown in Fig. 5, in which an initial crack length, *a*, of 1 μm has been considered for all cases.

These simulations prove that the assumed initial crack aspect ratio only affects the aspect ratio at any length for cracks smaller than 20 μm.

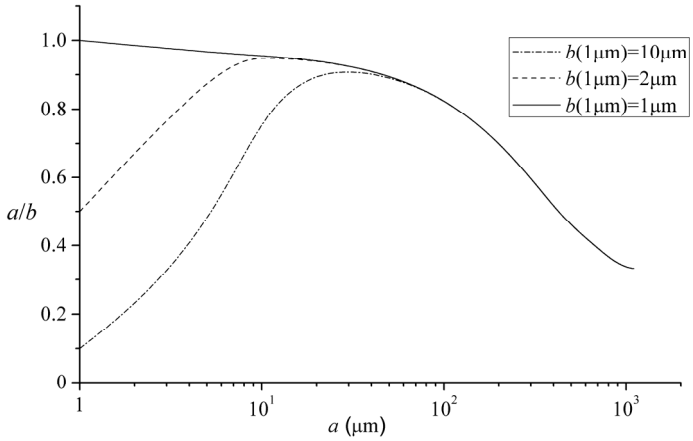

Figure 5: Crack aspect evolution for different initial crack aspect.

Crack initiation phase

To analyse the crack initiation phase, the fatigue model here applied takes ideas from the work of McClung et al. [14]. The first step is to obtain from smooth fatigue test specimens the fatigue curve $N^{smooth}(\Delta\varepsilon,a)$. This curve gives, as a function of the applied strain range, $\Delta\varepsilon$, the number of cycles needed to initiate a crack of length a in smooth test specimens. For each value of $\Delta\varepsilon$ and a, the number of fatigue cycles, $N^{smooth}(\Delta\varepsilon,a)$, is calculated as follows:

$$N^{smooth}\left(\Delta\varepsilon,a\right)=N_0^{smooth}\left(\Delta\varepsilon\right)-N_p^{smooth}\left(\Delta\varepsilon,a\right)=N_0^{smooth}\left(\Delta\varepsilon\right)-\int_a^{a_f}\frac{dl}{f\left(\Delta\varepsilon,l\right)} \tag{7}$$

In Eq. (7), $N_t^{smooth}(\Delta\varepsilon)$ represents the total number of fatigue cycles obtained in a smooth test specimen subjected to a strain range $\Delta\varepsilon$. $N_p^{smooth}(\Delta\varepsilon,a)$ is the number of cycles required to propagate the crack from a to the final fracture crack length, a_f, for a smooth test specimen subjected to $\Delta\varepsilon$. Finally, $f(\Delta\varepsilon,a)$ represents the fatigue crack growth law Eq. (1), in which ΔK_I is calculated according to the applied $\Delta\varepsilon$ and the geometry of the smooth fatigue test specimen. For the Al 7075-T651 alloy, the initiation curves $N^{smooth}(\Delta\varepsilon,a)$ for different initiation cracks lengths are represented in Fig. 6. The $N_t^{smooth}(\Delta\varepsilon)$ curve is also plotted in this figure.

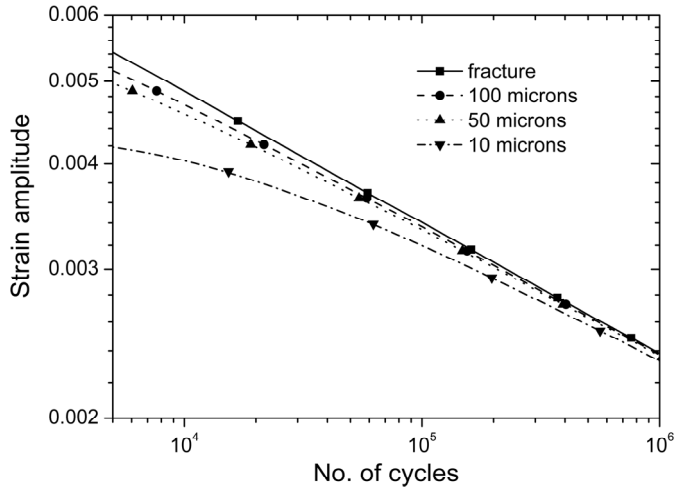

Figure 6: Initiation crack curves for Al 7075-T651 alloy.

In the case where a multi-axial stress/strain state and a stress/strain gradient are present, as in fretting fatigue, the same procedure can be applied, but with some changes. First, a multi-axial fatigue parameter should be used. In this work, the

Fatemi-Socie parameter (FS) has been used [15]. Using the set of $N^{smooth}(\Delta\varepsilon,a)$ curves, a new set of $N^{smooth}(FS,a)$ curves are obtained. However, in a fretting fatigue situation where a stress/strain gradient with depth is present, the FS parameter also varies with depth. Therefore, the crack initiation life depends on where the parameter is evaluated. Considering the results from previous works [16], the mean value of the FS parameter between the surface and a depth equal to the prospective crack initiation length, a, is considered the most appropriate option. With this average value and the set of $N^{smooth}(FS,a)$ curves, the number of cycles required to initiate a crack with a length equal to a is obtained. Because a mean value is used, the calculation is approximate in nature. With this option, it is the hypothesis that zones with the same mean value of the parameter require the same number of cycles to initiate a crack.

Combination of the crack initiation and crack propagation phases

When the curves $N_i(a)$ and $N_p(a)$ are acquired, these values are added to obtain a new curve $N_t(a)= N_i(a)+N_p(a)$, which gives the total number of fatigue cycles needed as a function of the assumed initial crack length, a. The value of a that minimises the total number of cycles is considered the *crack initiation length*. The minimum value of N_t is the fatigue life. This fatigue model presents the advantage that there is no need to determine a priori when the crack initiation phase finishes and, hence, when the crack propagation phase starts. The decision is made based on the value of a that minimises the total fatigue life N_t. Fig. 7 shows the curves $N_i(a)$, $N_p(a)$ and $N_t(a)$ obtained in a simulation of the test type 3, using a 3D model. The parameters defining this type of test will be shown further in this document. In the following figure, it is observed that the crack initiation length, i.e., the value of a that minimises N_t, is approximately equal to 65 μm.

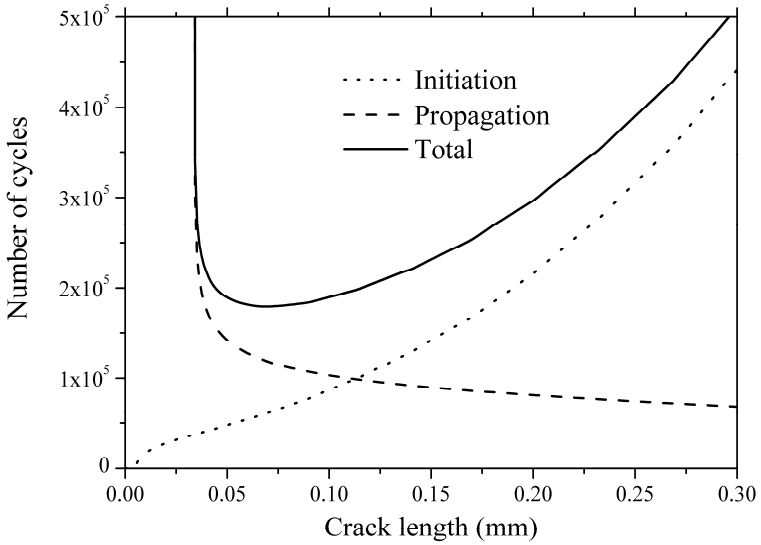

Figure 7: Curves $N_i(a)$, $N_p(a)$ and $N_t(a)$ obtained in a 3D simulation.

FATIGUE TESTS

Following the same procedure described in [11], a series of fretting fatigue tests were performed. The data for completed tests are shown in Tab. 1. Seven varying load combinations were applied to meet two main fretting fatigue test goals: completing tests with a wide range in fatigue lives and carrying out tests with varying predominate loads.

FATIGUE LIFE PREDICTIONS

The fretting fatigue life predictions were performed using the mechanical and fatigue properties for the Al 7075-T651, as shown in Tab. 2 [17]. In this table, the σ_f', b, ε_f' and c are parameters defining the $\Delta\varepsilon$-N curve, and the constants K' and n' define the stress-strain Ramberg-Osgood curve.

Test	Type	N(N)/Q(N)	σ(MPa)	N_{exp}
1	1	5800 / 850	40	1070886
2	1	5800 / 850	40	1793368
3	2	5800 / 850	50	577540
4	2	5800 / 850	50	382064
5	2	5800 / 850	50	676704
6	3	5800 / 1100	70	303509
7	3	5800 / 1100	70	347072
8	4	5800 / 1100	55	252878
9	4	5800 / 1100	55	283110
10	5	5800 / 1350	70	167324
11	5	5800 / 1350	70	165421
12	6	4750 / 1100	110	52440
13	6	4750 / 1100	110	57032
14	7	3690 / 1350	110	32395
15	7	3690 / 1350	110	57479

Table 1: Loads (N and Q), axial stress (σ) and experimental fatigue cycles (N_{exp}).

E	ν	σ_u	σ_y
70 GPa	0.33	572 MPa	503 MPa
C	n	ΔK_{th}	$\Delta\sigma_{FL}$
$8.83 \cdot 10^{-11}$	3.322	2.1 MPa√m	169 MPa
σ_f'	b	ε_f'	c
1231	-0.122	0.26	-0.806
K'	n'		
694 MPa	0.04		

Table 2: Mechanical and fatigue properties for the Al 7075-T651.

The fretting fatigue predictions obtained for the 2D (plane stress or plane strain) and 3D models, are shown in Tab. 3. In addition, Tab. 3 indicates the experimental lives.

To consider the full picture of the behaviour offered by each model (2Ds or 3D), Fig. 8 presents the predictions, N_{pred}, versus the experimental lives, N_{exp}, for all cases. This plot illustrates the solid predictions obtained using both 2D models; furthermore, it illustrates that both models provide similar predictions. Regarding the 3D model, this plot also indicates good behaviour; however, for test type 2, the results were worse than those obtained using the 2D models.

To complete the prediction obtained using the models, Fig. 9 represents the percentage of N_i and the crack initiation length as a function of the predicted life N_{pred}. This plot shows that the crack initiation lengths are continuously longer than 20 μm, justifying the low influence exerted on the fatigue predictions by the assumed initial crack aspect ratio. Similarly, this plot displays that the comparative relevance of both the crack initiation and the crack propagation phases can vary across test results. This fact shows that it is not possible to ignore either the crack initiation phase or the crack propagation phase when conducing these tests. Finally, Fig. 9 also indicates that the crack initiation length is always shorter than 70 μm; a model that considers the short crack growth phase is expedient.

Type	N_{exp}	Plane stress	Plane strain	3D
1	1070886 1793368	949195	876623	1997908
2	577540 382064 676704	564307	530292	1017824
3	303509 347072	150253	132687	179496
4	252878 283110	236057	205330	294700
5	167324 165421	94757	87313	104212
6	52440 57032	67845	61666	69356
7	32395 57479	55983	51213	48948

Table 3: Fretting fatigue life predictions.

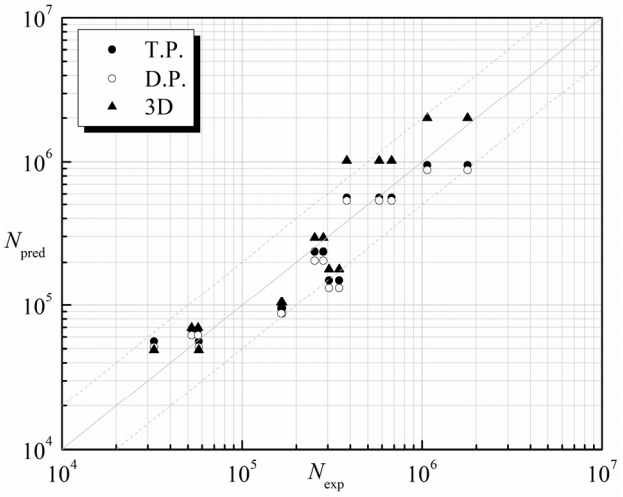

Figure 8: N_{pred} vs. N_{exp}.

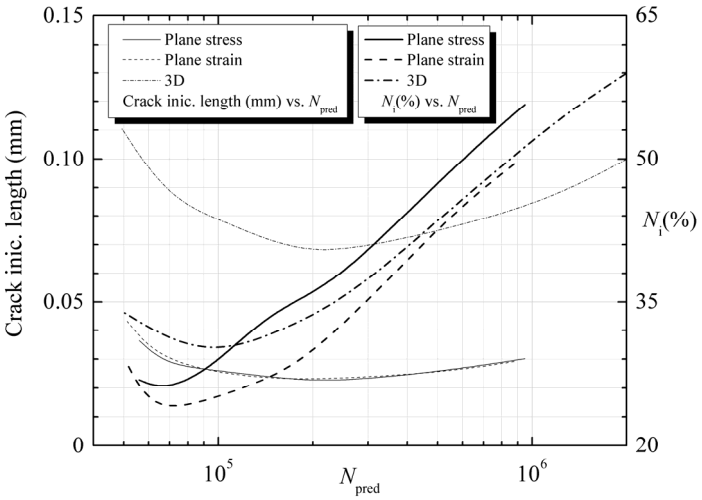

Figure 9: Crack initiation length vs. N_{pred} and N_i(%) vs. N_{pred}.

Conclusions

In this work, the effect that the model's geometry has on the fretting fatigue life predictions has been studied. For the cylinder-plane contact pair considered, all of the models give similar results. These results are proven to be virtually identical in the 2D cases. These results additionally justify the use of a 2D FEM that provides the advantage of lower computational cost compared with 3D models.

References

[1]Waterhouse, R.B., Fretting Fatigue, Applied Science Publisher, (1981).
[2]Nishioka, K., Hirakawa, K., Fundamental investigation on fretting fatigue—part 4. The effect of mean stress, Bull. Jpn. Soc. Mech. Eng., 12 (1969) 408–414.

[3]Navarro, C., Muñoz, S., Domínguez, J., Propagation in fretting fatigue from a surface defect, Tribol. Int., 39 (2006) 1149–1157.
[4]Hattori, T., Kien, V.T., Yamashita, M., Fretting fatigue life estimations based on fretting mechanisms, Tribol. Int., 44 (2011) 1389–1393.
[5]Hills, D.A. et al., Correlation of fretting fatigue experimental results using an asymptotic approach, Int. J. Fat., 43 (2012) 62–75.
[6]Szolwinski M., Farris T., Observation, analysis and prediction of fretting fatigue in 2024-T351 aluminum alloy, Wear, 221 (1998) 24–36.
[7]Navarro, C., García, M., Domínguez, J., A procedure for estimating the total life in fretting fatigue, Fat. Fract. Engng. Mater. Struct., 26 (2003) 459-468.
[8]Socie D.F., Morrow, J., Chen, W.C., A procedure for estimating the total fatigue life of notched and cracked members, Engng. Fract. Mech., 11 (1979) 851-859.
[9]Muñoz, S., Navarro, C., Domínguez, J., Application of fracture mechanics to estimate fretting fatigue endurance curves, Engng. Fract. Mech., 74 (2007) 2168-2186.
[10]Vallellano, C., Domínguez, J., Navarro, A., On the estimation of fatigue failure under fretting conditions using notch methodologies, Fat. Fract. Engng. Mater. Struct., 26 (2003) 469-478.
[11]Tam, R. et al., Caracterización de una máquina para realizar ensayos de fretting fatiga con contacto cilíndrico, Anales de la mecánica de la fractura, (2011) 323-328.
[12]Orynyak, I.V., Borodii, M.V., Torop, V.M., Approximate Construction of a Weight Function for Quarter-Elliptical, Semi-Elliptical and Elliptical Cracks Subjected to Normal Stresses. Eng. Fract. Mech., 49 (1994) 143-151.
[13]Bueckner, H.J., Sih, G.C. (Ed.), Methods of analysis and solutions of crack problems, Noordhoff Int. Publishing, (1973).
[14]McClung, RC, Francis, WL, Hudak, Jr. SJ, A new approach to fatigue life prediction based on nucleation and growth. In: 9th International fatigue congress, Atlanta, 2006.
[15]Fatemi, A. Socie, D. A., Critical plane approach to multiaxial fatigue damage including out-of-phase loading, Fatigue. Fract. Eng. Mater. Struct., 11 (1998) 145–65.
[16]Navarro, C., Muñoz, S., Domínguez, J., Influence of the initiation length in predictions of life in fretting fatigue, Strain, 47 (2011) 283–91.
[17]Navarro, C., Vázquez, J., Domínguez, J., 3D vs. 2D fatigue crack initiation and propagation in notched plates, Int. J. Fat, 58 (2014) 40-46.